




Attitude Control of Active Suspension All-Terrain Vehicle Based on LQR

Liang Wu^{1,3}, Shucheng Li¹, Guangjian Xu¹, Weizhou Zhang¹, and Weiwei Jia²

¹ The State Key Laboratory of Automotive Simulation and Control (Jilin University),
Changchun, China

astdwxg@jlu.edu.cn

² Jilin University of Finance and Economics, Changchun, China

³ Changsha Automotive Innovation Research Institute, Changsha, China

Abstract. In order to enhance the attitude control ability of all-terrain vehicles in complex terrain, a dual closed-loop control strategy based on LQR controller is designed with series active suspension all-terrain vehicles as the research object. Firstly, considering the kinematic and dynamic relationships between each mechanism of the all-terrain vehicle, a vehicle dynamic model based on the speed control of the actuator is constructed on the basis of the traditional active suspension force control. Secondly, a terrain estimation algorithm based on all-terrain vehicle model is studied, and a LQR controller suitable for attitude adjustment is designed. Finally, three pavement models are established to simulate real road conditions for verifying the accuracy of the dynamic model with terrain estimation model and the effectiveness of attitude control. The results show that the collaborative control strategy proposed in this paper has good adaptability to working conditions, and the peak and Root mean square values of vertical displacement, pitch angle and roll angle of all-terrain vehicle body are reduced by 30–50%, which can greatly improve the ride comfort and attitude stability of all-terrain vehicle.

Keywords: all-terrain vehicle · active suspension · LQR · attitude control

1 Introduction

For the practical needs of resource exploration, military combat, post-disaster search, rescue and fire-fighting, etc., all-terrain vehicles have the ability to travel flexibly in complex geological environments, so it is a major research hotspot in the industry [1].

The above capabilities can rely on active suspension for attitude control [2], which can adjust the whole vehicle attitude to improve the ride and handling stability of the vehicle according to the current motion condition of the vehicle, terrain undulation [3, 4], etc. As a kind of limited bandwidth active suspension, the response frequency of series active suspension is lower than that of full bandwidth active suspension, generally below about 5 Hz, which can save energy consumption. Compared with the parallel and hybrid active suspension, the series suspension is simpler in structure, lower in design cost, and has a larger attitude adjustment range, which is of good research significance for all-terrain vehicles [5, 6].

In recent years, many domestic and foreign scholars have used a variety of algorithms to control the suspension, including optimal control, adaptive control, preview control, fuzzy control, robust control, sliding mode control, neural network control and so on [7–13]. The LQR (linear quadratic regulator) adopted in this paper is a kind of optimal control applied in linear system, different state feedback matrices \mathbf{K} can be obtained by adjusting the weighting coefficient matrices \mathbf{Q} and \mathbf{R} , which also represents different control laws, and a closed-loop optimal control system can be obtained according to the actual requirements, which can satisfy the multiple performance indicators of the all-terrain vehicles [14].

The focus of this paper is to improve the attitude control ability of all-terrain vehicle in complex terrain based on series active suspension. Firstly, the motion equations are established sequentially according to the kinematic and dynamic relationships between each mechanism of the all-terrain vehicle, a vehicle modeling method based on the speed control of the actuator is studied on the basis of the traditional active suspension force control, and a vehicle dynamics model is constructed by jointly integration; secondly, a terrain estimation algorithm based on all-terrain vehicle model is studied, and a LQR controller suitable for attitude adjustment is designed, the controller is simulated with the vertical acceleration, vertical displacement, roll angle and pitch angle of the all-terrain vehicle as the performance indicators, and the terrain for verifying the simulation performance of the attitude control is designed, so as to verify the accuracy of the dynamic model with terrain estimation model and the effectiveness of attitude control.

2 Vehicle Dynamic Model

Figure 1 shows a whole vehicle dynamics model of the ATV, which can be divided into five parts: a vehicle body and four series active suspensions.

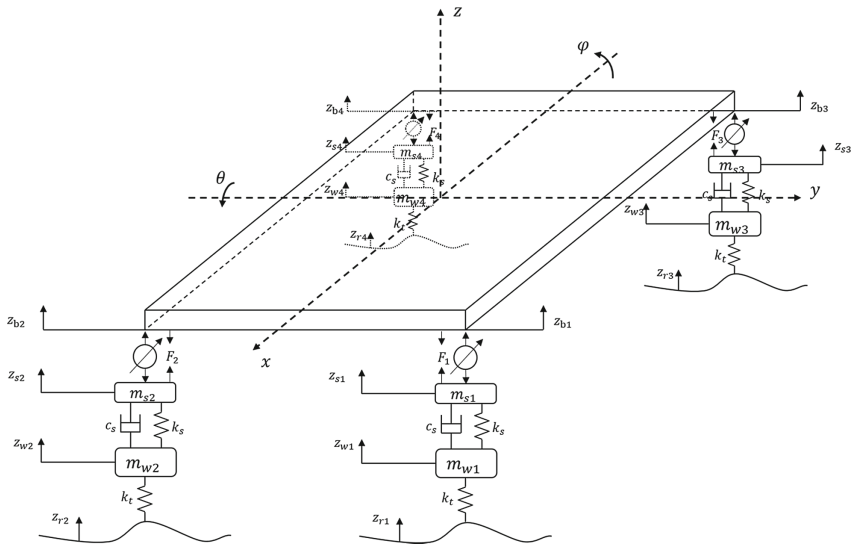


Fig. 1. Dynamic model of an all-terrain vehicle

Considering the body as a rigid body, its upward vertical runout, forward or backward pitch, and left or right roll can be expressed by Eq. (1–3).

$$m_b \ddot{z} = F_1 + F_2 + F_3 + F_4 \quad (1)$$

$$I_p \ddot{\theta} = (F_3 + F_4)b - (F_1 + F_2)a \quad (2)$$

$$I_r \ddot{\varphi} = (F_1 - F_2) \times \frac{1}{2} B_f + (F_3 - F_4) \times \frac{1}{2} B_r \quad (3)$$

where m_b is the mass of the body; z is the vertical displacement of the body; \ddot{z} is the vertical acceleration of the body; θ and φ are the pitch and roll angles of the body; a and b are the distance from the front and rear axles to the centre of mass respectively; B_f and B_r are the front and rear wheelbases; $F_{1\sim 4}$ is the control force of the four actuators respectively; and I_p and I_r are the rotational inertia of the body for pitching and rolling. Meanwhile, since the roll angle and pitch angle are small variations in real situations, the body attitude can be decomposed into vertical displacements at the four endpoints by Eq. (4).

$$\begin{aligned} z_{b1} &= z - a\theta + \frac{1}{2} B_f \varphi \\ z_{b2} &= z - a\theta - \frac{1}{2} B_f \varphi \\ z_{b3} &= z + b\theta + \frac{1}{2} B_r \varphi \\ z_{b4} &= z + b\theta - \frac{1}{2} B_r \varphi \end{aligned} \quad (4)$$

where $z_{b1\sim b4}$ are the vertical displacements at the four endpoints of the vehicle. The vertical motion equations of the wheels at each suspension and those of each actuator support block are given by Eq. (5) and (6).

$$m_{wi} \ddot{z}_{wi} = c_s (\dot{z}_{si} - \dot{z}_{wi}) + k_s (z_{si} - z_{wi}) + k_t (z_{ri} - z_{wi}), i = 1, 2, 3, 4 \quad (5)$$

$$m_{si} \ddot{z}_{si} = c_s (\dot{z}_{wi} - \dot{z}_{si}) + k_s (z_{wi} - z_{si}) - F_i, i = 1, 2, 3, 4 \quad (6)$$

where $m_{w1\sim w4}$ are the masses of the four wheels; $m_{s1\sim s4}$ are the masses of the support blocks connecting each actuator; c_s is the damping of each suspension; k_s is the stiffness of each damper; $z_{s1\sim s4}$ are the vertical displacements of each actuator; k_t is the stiffness of each tire; $z_{w1\sim w4}$ are the vertical displacements of each wheel; $z_{r1\sim r4}$ are the road excitation of each wheel. It is known that the actuator support block in the middle position of the suspension only plays a guiding role, and the mass of the support block is small, so the mass of the support block can be ignored in order to further simplify the model, as shown in Fig. 2.

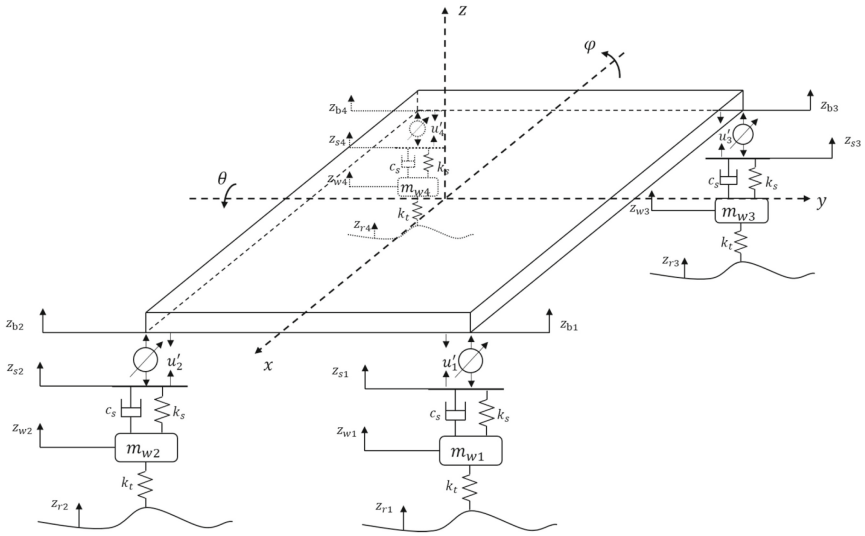


Fig. 2. Simplified vehicle dynamic model

The control force of the four electric servo actuators can be expressed as

$$F_i = c_s(\dot{z}_{wi} - \dot{z}_{si}) + k_s(z_{wi} - z_{si}), i = 1, 2, 3, 4 \tag{7}$$

Substituting into Eq. (1-3), and the input of the actuator displacement can be expressed as

$$u'_i = z_{bi} - z_{si}, i = 1, 2, 3, 4 \tag{8}$$

Since there are no parallel dampers in the actuators of the series active suspension to provide the relationship between the upper and lower velocities, and there are no additional sensors to provide the corresponding state data, it is difficult to use the actuator forces for attitude control, so a second-order low-pass filter (LPF) [15] is introduced for each actuator to achieve velocity control based on the force control transition, as shown in Fig. 3.

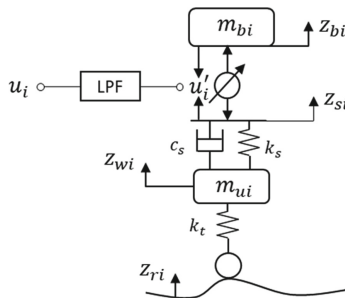


Fig. 3. Series active suspension with LPF

The equation of LPF is

$$\ddot{u}'_i + 2\zeta\omega_c\dot{u}'_i + \omega_c^2u'_i = u_i, i = 1, 2, 3, 4 \quad (9)$$

where, ω_c is the cut-off frequency of the suspension; ζ is the damping ratio of the suspension; u_i is the control displacement input calculated without low-pass filtering; u'_i is the control displacement input, which is the actual action to the suspension, and ultimately the control velocity \dot{u}'_i of the actuator can be obtained.

In summary, the state variable \mathbf{x} , control input \mathbf{u} , road input variable \mathbf{w} , and output vector \mathbf{y} are obtained.

$$\mathbf{x} = [\dot{z}_b, \dot{\theta}, \dot{\phi}, z, \theta, \phi, \dot{z}_{w1\sim w4}, z_{w1\sim w4}, \dot{u}'_{1\sim 4}, u'_{1\sim 4}]^T \quad (10)$$

$$\mathbf{u} = [u_1, u_2, u_3, u_4]^T \quad (11)$$

$$\mathbf{w} = [z_{r1}, z_{r2}, z_{r3}, z_{r4}]^T \quad (12)$$

$$\mathbf{y} = [\ddot{z}, z, \theta, \phi, \Delta_{s1\sim s4}, \dot{u}'_{1\sim 4}, u'_{1\sim 4}]^T \quad (13)$$

The system state space equation is

$$\begin{cases} \dot{\mathbf{x}} = \mathbf{A}\mathbf{x} + \mathbf{B}\mathbf{u} + \mathbf{D}\mathbf{w} \\ \mathbf{y} = \mathbf{C}\mathbf{x} \end{cases} \quad (14)$$

where \mathbf{A} is a $n_x \times n_x$ dimensional matrix, \mathbf{B} is a $n_x \times n_u$ dimensional matrix, \mathbf{D} is a $n_x \times n_w$ dimensional matrix, \mathbf{C} is a $n_y \times n_x$ dimensional matrix, $n_x = 22$, $n_u = 4$, $n_w = 4$, $n_y = 16$.

3 LQR Controller Design

Controller design is carried out for the established dynamic model, including pavement modeling, terrain estimation and attitude control.

3.1 Pavement Model

The working road conditions of the all-terrain vehicle are relatively harsh. Three kinds of road models are established to simulate the real road conditions. Because of the need to control the vehicle's pitch and roll, only the left wheel is stimulated in the simulation environment, and the right wheel is not stimulated.

3.1.1 Bump Pavement

The bump pavement is mainly used to reflect the response of a vehicle when it passes through the speed bump or bump bulge. According to GB/T4970-2009 [16], the mathematical model of the bump pavement is established:

$$z_r(t) = \begin{cases} 0, & 0 \leq t \leq \frac{l}{v} \\ \frac{A_L}{2}(1 - \cos(\frac{2\pi v}{L}t)), & \frac{l}{v} \leq t \leq \frac{l+L}{v} \\ 0, & t > \frac{l+L}{v} \end{cases} \quad (15)$$

where $z_r(t)$ is the vertical elevation of the bump pavement in m; l is the distance from the wheels to the front end of the speed bump in m; v is the travelling speed of the vehicle in m/s; A_L is the height of the speed bump in m; and L is the width of the speed bump in m. $A_L = 0.05$ m and $L = 0.6$ m, as shown in Fig. 4.

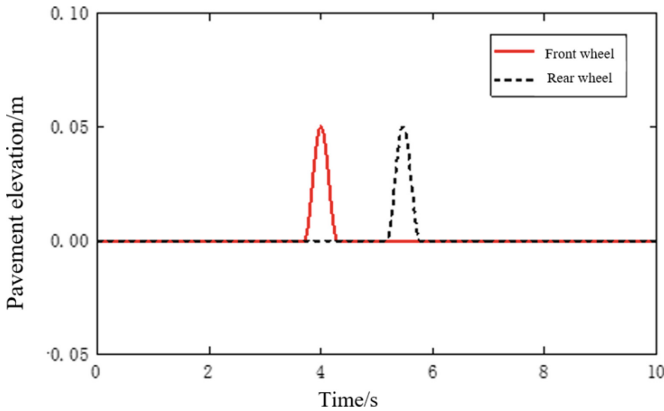


Fig. 4. Left front and rear wheels bump pavement excitation

3.1.2 Sinusoidal Wave Pavement

The sinusoidal pavement is mainly used to reflect the response of a vehicle when it is impacted by a continuous waveform. The amplitude of the sinusoidal wave is determined to be 0.08 m, the vehicle speed is 1 m/s, and the period is 2 s, as shown in Fig. 5.

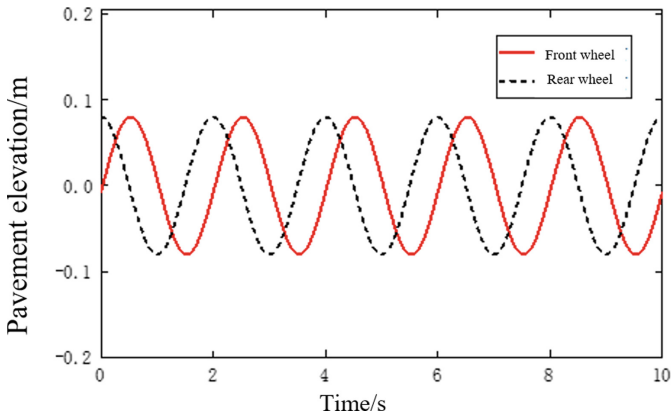


Fig. 5. Left front and rear wheels sinusoidal pavement excitation

3.1.3 Random Pavement

Random pavement shows the changes of the road surface, according to the ISO/TC108/SC2N67 document and GB/T7031-1986 *Vehicle Vibration-Describing Method for Road Surface Irregularity* standard, the D-class random pavement conditions are selected for simulation. The road surface Irregularity coefficient is $1024 \times 10^{-6} \text{ m}^2/\text{m}^{-1}$, the vehicle speed is 1 m/s, and the lower cut-off frequency is 0.011 Hz, as shown in Fig. 6.

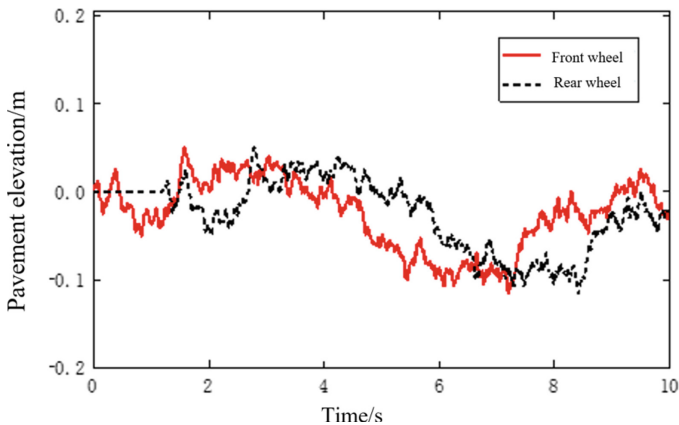


Fig. 6. Left front and rear wheels D-class pavement excitation

3.2 Terrain Estimation Algorithm

In attitude control of an all-terrain vehicle, it is necessary to obtain elevation information of the terrain in real time. Since it is not possible to rely on external sensors to predict the forward terrain information, terrain estimation algorithm based on kinetic models fused with existing sensors is investigated.

The sensor system of the ATV consists of LPMS attitude sensors, draw-wire displacement sensors, travel and speed sensors with the electric servo actuators. Among them, the LPMS attitude sensors can monitor the attitude angles of the ATV body, including the pitch angle and the roll angle; the draw-wire displacement sensors are installed at the upper and lower ends of the passive damper, four in all, which can measure the real-time passive suspension dynamic travel of the air-spring damper; and the sensors of the electric servo actuators on the four series active suspensions can feed back real-time actuator elongation and speed.

In summary, considering the established ATV dynamic model and the existing sensors, there are nine attitude states of the ATV changes when it is disturbed by the terrain: forward pitch and left roll, forward pitch and right roll, backward pitch and left roll, backward pitch and right roll, forward pitch only, backward pitch only, left roll only, right roll only, and balanced posture. Figure 7 shows the deduced terrain estimation model.

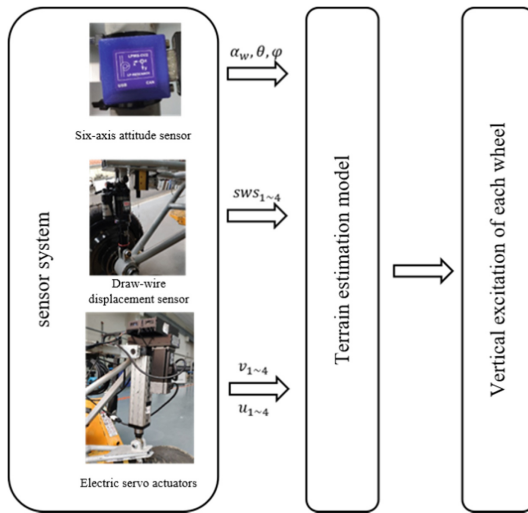


Fig. 7. Terrain estimation model based on the whole vehicle sensor system

The real-time ATV state information obtained by the sensor system are: body vertical acceleration a_w , body pitch angle θ , body roll angle ϕ , velocity of each actuator $v_{1\sim4}$, displacement of each actuator $u'_{1\sim4}$, and passive suspension dynamic travel measured by each draw-wire displacement sensor $SWS_{1\sim4}$. Since the value of body vertical displacement z is difficult to be measured, the terrain information at each wheel $w_{1\sim4}$ are estimated based on the 15 quantities measured by the above sensor system.

The vertical displacement at the center of mass of the vehicle body is estimated based on the followed eight body attitude states:

- (1) When the body attitude is forward pitch and right roll ($(\theta < 0) \cap (\phi > 0)$),

$$z = -a \sin \theta + B_f \sin \phi + SWS_4 + u'_4 \tag{16}$$

- (2) When the body attitude is backward pitch with right roll and only right roll $((\theta \geq 0) \cap (\phi > 0))$,

$$z = a \sin \theta + B_f \sin \phi + SWS_2 + u'_2 \quad (17)$$

- (3) When the body attitude is forward pitch with left roll and only forward pitch $((\theta < 0) \cap (\phi \leq 0))$,

$$z = -a \sin \theta - B_f \sin \phi + SWS_3 + u'_3 \quad (18)$$

- (4) When the body attitude is backward pitch with left roll, only backward pitch, only left roll and balanced posture $((\theta \geq 0) \cap (\phi \leq 0))$,

$$z = a \sin \theta - B_f \sin \phi + SWS_1 + u'_1 \quad (19)$$

The vertical displacement at each end point of the body $z_{b1 \sim b4}$ is obtained by substituting into Eq. (4):

$$w_i = z_{bi} - SWS_i - u'_i - DTD_i, i = 1, 2, 3, 4 \quad (20)$$

where $DTD_{1 \sim 4}$ is the tire dynamic displacement of each wheel, which can be ignored because of its small value compared to that of the road, so the equation is:

$$w_i = z_{bi} - SWS_i - u_i, i = 1, 2, 3, 4 \quad (21)$$

Finally, the vertical displacement excitation acting on each wheel w is obtained according to Eq. (22), which means the estimated terrain is obtained.

$$\mathbf{w} = \begin{bmatrix} w_1 \\ w_2 \\ w_3 \\ w_4 \end{bmatrix} \quad (22)$$

3.3 LQR Attitude Controller

LQR is a kind of optimal control applied in linear system, which can adjust the weighting coefficients according to the actual requirements to obtain a closed-loop optimal control system. The factors affecting the body attitude of an all-terrain vehicle are: body vertical acceleration, roll angle, pitch angle, dynamic travel of the passive suspension and dynamic tire displacement. The cost function of the active attitude control LQR for the all-terrain vehicle is

$$J = \rho_1 (\ddot{z}^2) + \rho_2 (z) + \rho_3 (\theta) + \rho_4 (\varphi) + \rho_5 \sum_{j=1}^4 \Delta_{sj}^2 + \rho_6 \sum_{j=1}^4 \Delta_{ij}^2 + \rho_R \sum_{j=1}^4 u_j^2 \quad (23)$$

where, ρ_1 is the weighting coefficient of the vertical displacement acceleration \ddot{z} of the ATV body; ρ_2 is the weighting coefficient of the vertical runout z of the ATV body;

ρ_3 is the weighting coefficient of the pitch angle θ of the ATV; ρ_4 is the weighting coefficient of the roll angle ϕ of the ATV; ρ_5 is the weighting coefficient of the dynamic travel Δ_{sj} of the passive damper of the ATV; ρ_6 is the weighting coefficient of the tire displacement Δ_{ij} of the ATV; ρ_R is the weight coefficient of the control input of the all-terrain vehicle. It is possible to derive different control laws which have different weights for various aspects of performance by changing the weight coefficients. The dynamic tire displacement Δ_{ij} and the dynamic travel Δ_{sj} of the passive suspension are expressed as

$$\sum_{j=1}^4 \Delta_{ij}^2 = (z_{w1} - z_{r1})^2 + (z_{w2} - z_{r2})^2 + (z_{w3} - z_{r3})^2 + (z_{w4} - z_{r4})^2 \quad (24)$$

$$\sum_{j=1}^4 \Delta_{sj}^2 = (z_{b1} - z_{w1})^2 + (z_{b2} - z_{w2})^2 + (z_{b3} - z_{w3})^2 + (z_{b4} - z_{w4})^2 \quad (25)$$

Assuming the output state is

$$\mathbf{y} = \mathbf{C}\mathbf{x} \quad (26)$$

Which includes all the variables that need to be constrained, such as tire dynamic displacement, suspension dynamic travel, pitch and roll angle, etc. \mathbf{C} is the output matrix, which can be divided into two sub-matrices, \mathbf{C}_1 and \mathbf{C}_2 , $\mathbf{C} = [\mathbf{C}_1 \mathbf{C}_2]$.

The system can be defined as an infinite time linear constant system. Taking the initial operating moment of the system as 0, then the quadratic performance index of the system at this time can be simplified as

$$J = \int_0^{\infty} (\mathbf{y}^T \mathbf{Q} \mathbf{y} + \mathbf{u}^T \mathbf{R} \mathbf{u}) dt \quad (27)$$

where $\mathbf{Q}(n_x \times n_x)$ and $\mathbf{R}(n_u \times n_u)$ are weighting coefficient matrixes, \mathbf{Q} is a positive semidefinite matrix and \mathbf{R} is a positive definite matrix. According to the optimal control theory, Eq. (28) can be obtained by solving Eq. (23)

$$\mathbf{u} = -\mathbf{K}\mathbf{x} = -\mathbf{R}^{-1} \mathbf{B}^T \mathbf{P} \mathbf{x} \quad (28)$$

where \mathbf{P} is a positive definite solution of the Riccati equation [17]

$$\mathbf{P}\mathbf{A} + \mathbf{A}^T \mathbf{P} - \mathbf{P}\mathbf{B}\mathbf{R}^{-1} \mathbf{B}^T \mathbf{P} + \mathbf{Q} = 0 \quad (29)$$

So the closed-loop state matrix equation is

$$\dot{\mathbf{x}} = (\mathbf{A} - \mathbf{B}\mathbf{K})\mathbf{x} + \mathbf{D}\mathbf{w} \quad (30)$$

4 Simulation and Analysis

Based on the above analysis, a dual closed-loop attitude control flowchart based on the LQR algorithm is shown in Fig. 8. The outer loop includes the real vehicle, actuators, and sensor system, and the inner loop includes the terrain estimation algorithm and the

LQR attitude controller. The linkage between the inner and outer loops is as follows: the outer loop ATV attitude adjustment is under the action of the electric servo actuators, and the whole vehicle system state is measured by the sensor system, then the terrain estimation algorithm obtains the road excitation, which is combined with the dynamic model established in the inner loop, then the control input is obtained through the calculation of LQR attitude controller and the control speed is obtained, which is acted to the electric servo actuator to satisfy the attitude control.

The three pavement models established in the previous paper are used to simulate real road conditions to verify the transient, stable state and random response characteristics of the control system respectively. The attitude stability (body vertical displacement, pitch angle and roll angle) and ride comfort (body vertical acceleration) of the ATV model are investigated by combining the terrain estimation with the LQR attitude controller.

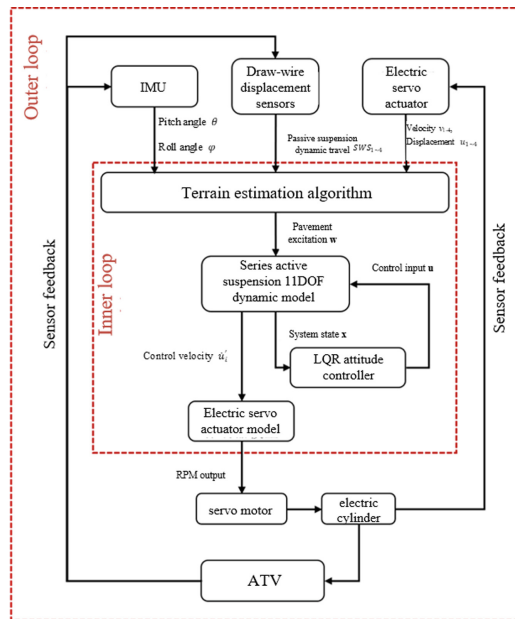


Fig. 8. Attitude control flowchart

The driving speed of the ATV in the simulation environment is set to be 1 m/s, the sampling frequency of the system is 100 Hz, and the simulation parameters are shown in Table 1.

Table 1. Detailed parameters of all-terrain vehicle

Parameters	Parameter symbol	Value	Unit
Vehicle body mass	m_b	150	kg
Single wheel mass	m_w	10	kg
Pitch moment of inertia	I_p	20.29	$\text{kg} \cdot \text{m}^2$
Roll moment of inertia	I_r	16.2	$\text{kg} \cdot \text{m}^2$
Distance from front axle to center of mass	a	0.65	m
Distance from rear axle to center of mass	b	0.65	m
Wheelbase	B_f, B_r	1.2	m
Damper stiffness	k_s	14319	N/m
Tire stiffness	k_t	200000	N/m
Damper damping coefficient	C_s	1479	$\text{N} \cdot \text{s/m}$
Cut-off frequency	ω_c	1.5	Hz
Damping ratio	ζ	0.7071	—
Maximum actuator travel	u_{max}	0.2	m
Maximum actuator speed	\dot{u}_{max}	0.125	m/s
Rated actuator force	F	2000	N

The weighting coefficients shown in Table 2 were selected by combining the parameters such as the vertical acceleration and the vertical displacement at the center of mass of the body of the all-terrain vehicle. Among them, passive suspension (PS) represents no attitude control, i.e., the actuator does not work; LQR attitude control system (LQRS) represents LQR attitude control based on the whole vehicle dynamic model.

Table 2. Values of weighting coefficients of LQR attitude controller

Weighting coefficients	ρ_1	ρ_2	ρ_3	ρ_4	ρ_5	ρ_6	ρ_R
PS	0	0	0	0	10	1	0
LQRS	1	1×10^4	1×10^4	1×10^4	100	1	3.5×10^{-8}

4.1 Simulation Results of Bump Pavement

The simulation results of the ATV on the bump pavement are shown in Fig. 9.

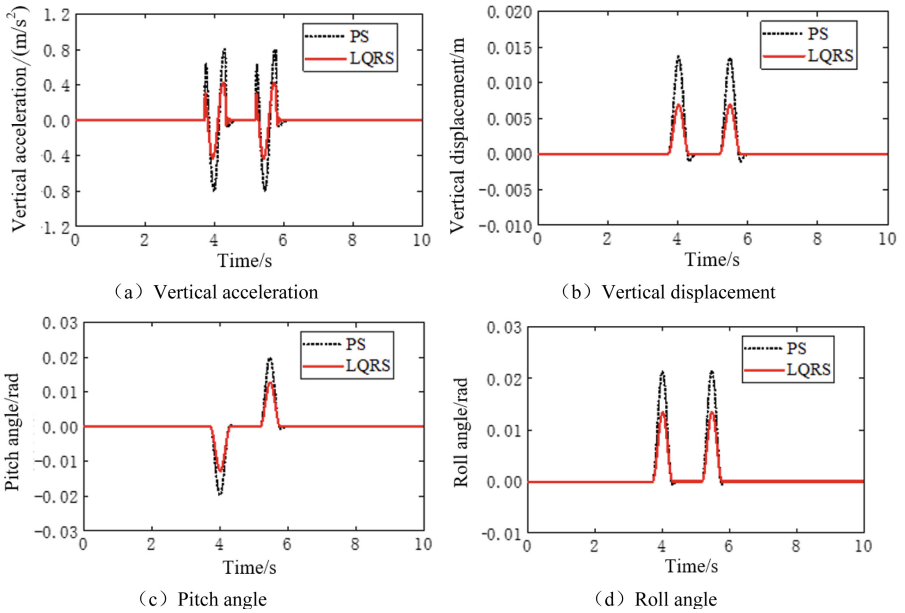


Fig. 9. Simulation results of bump pavement

As shown in Table 3, the peak reduction ratios of vertical acceleration, vertical displacement, pitch angle and roll angle of all-terrain vehicle in response to bump pavement impacts are 46.99%, 49.26%, 35.86% and 37.21%, respectively. The root mean square (rms) value reduction ratios are 46.58%, 46.43%, 35.71% and 35.56%, respectively. The validity of the established dynamic model, terrain estimation model and LQR attitude controller is verified, and it also shows that the controller can effectively improve the ride comfort and attitude stability of the ATV when it copes with transient impacts.

Table 3. Comparison of attitude control simulation results of bump pavement

Performance indicators	Peak value			Rms value		
	PS	LQRS	Reduction ratios	PS	LQRS	Reduction ratios
vertical acceleration/(m/s ²)	0.8063	0.4274	46.99%	0.1945	0.1039	46.58%
vertical displacement/m	0.0136	0.0069	49.26%	0.0028	0.0015	46.43%
pitch angle/rad	0.0198	0.0127	35.86%	0.0042	0.0027	35.71%
roll angle/rad	0.0215	0.0135	37.21%	0.0045	0.0029	35.56%

4.2 Simulation Results of Sinusoidal Wave Pavement

The simulation results of the ATV on the sinusoidal wave pavement are shown in Fig. 10.

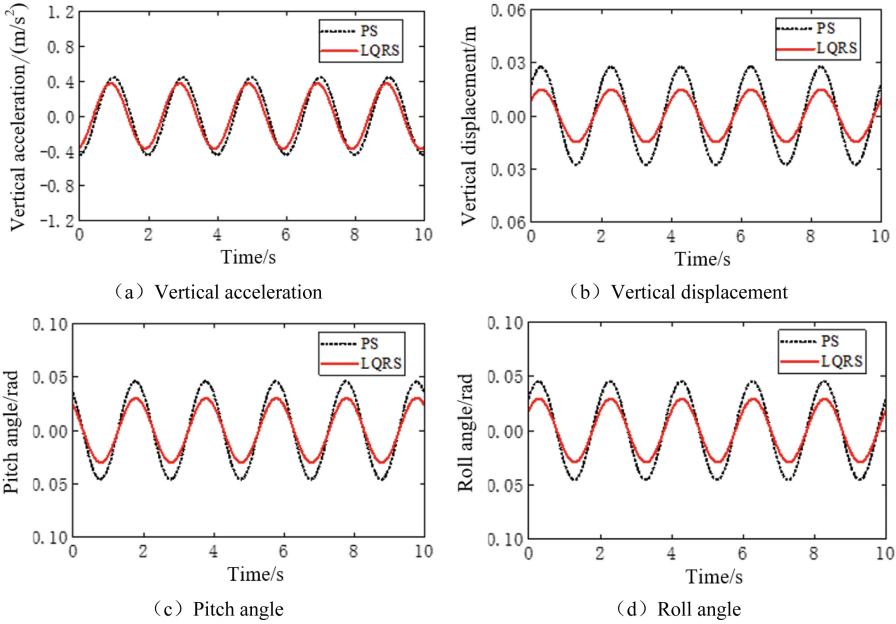


Fig. 10. Simulation results of sinusoidal wave pavement

As shown in Table 4, the peak reduction ratios of vertical acceleration, vertical displacement, pitch angle and roll angle of all-terrain vehicle in response to sinusoidal wave pavement impacts are 15.6%, 46.38%, 34.35% and 35.76%, respectively. The rms value reduction ratios are 15.62%, 46.15%, 34.37% and 35.63%, respectively. It shows that the controller can improve the ride comfort and attitude stability of the ATV when it is responding to continuous impacts, but the improvement in ride comfort is smaller compared to that of bump pavements.

Table 4. Comparison of attitude control simulation results of sinusoidal wave pavement

Performance indicators	Peak value			Rms value		
	PS	LQRS	Reduction ratios	PS	LQRS	Reduction ratios
vertical acceleration/(m/s ²)	0.4417	0.3728	15.60%	0.3125	0.2637	15.62%
vertical displacement/m	0.0276	0.0148	46.38%	0.0195	0.0105	46.15%
pitch angle/rad	0.0457	0.0300	34.35%	0.0323	0.0212	34.37%
roll angle/rad	0.0453	0.0291	35.76%	0.0320	0.0206	35.63%

4.3 Simulation Results of Random Pavement

The simulation results of the ATV on the random pavement are shown in Fig. 11. The peak reduction ratios of vertical acceleration, vertical displacement, pitch angle and roll angle of all-terrain vehicle in response to sinusoidal wave pavement impacts are 9.54%, 45.56%, 40.34% and 36.39%, respectively. The rms value reduction ratios are 10.47%, 45.33%, 35.22% and 35.67% respectively, as shown in Table 5.

It is shown that the controller is able to improve the ride comfort and attitude stability of the ATV when it copes with random pavement, but the improvement in ride comfort is smaller than that of attitude stability.

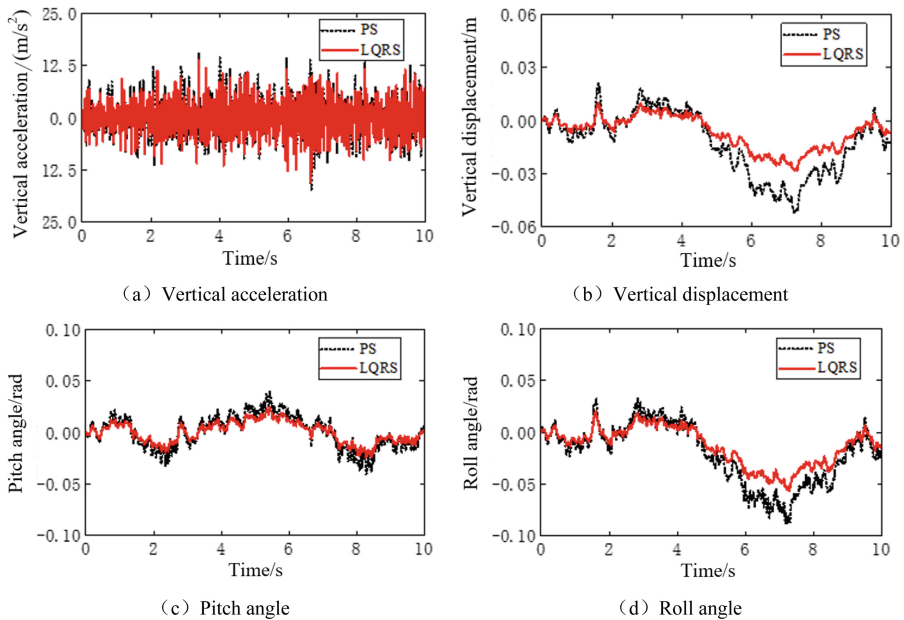


Fig. 11. Simulation results of random pavement

Table 5. Comparison of attitude control simulation results of random pavement

Performance indicators	Peak value			Rms value		
	PS	LQRS	Reduction ratios	PS	LQRS	Reduction ratios
vertical acceleration/(m/s ²)	17.498	15.829	9.54%	4.6293	4.1446	10.47%
vertical displacement/m	0.0518	0.0282	45.56%	0.0214	0.0117	45.33%
pitch angle/rad	0.0409	0.0244	40.34%	0.0159	0.0103	35.22%
roll angle/rad	0.0882	0.0561	36.39%	0.0356	0.0229	35.67%

The average simulation results of the ATV on the above three pavements are shown in Table 6, the average peak values of body vertical displacement, pitch angle and roll angle are reduced by 47.07%, 36.85% and 36.45%, the corresponding average reduction ratios of the root mean square value reach 45.97%, 35.10% and 35.62%, which shows that the control effect of the whole vehicle attitude is obvious. The reduction ratio of vertical acceleration reaches 24%, which indicates that the ride comfort of the vehicle has been improved to a certain extent, but the improvement for continuous impact and random vibration is relatively small.

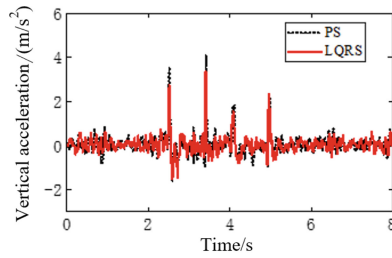
Table 6. Simulation results of the average reduction ratio of peak and rms values of three road surfaces

Performance indicators	Average reduction ratio of peak value	Average reduction ratio of rms value
vertical acceleration/(m/s ²)	24.04%	24.22%
vertical displacement/m	47.07%	45.97%
pitch angle/rad	36.85%	35.10%
roll angle/rad	36.45%	35.62%

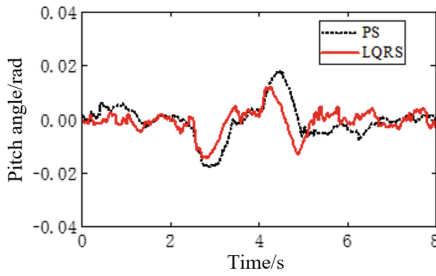
Overall, the vehicle dynamic model established in this paper, the terrain estimation model, and the corresponding LQR control strategy are simulated and verified, and relatively satisfactory results are achieved.

5 Experiments and Analysis

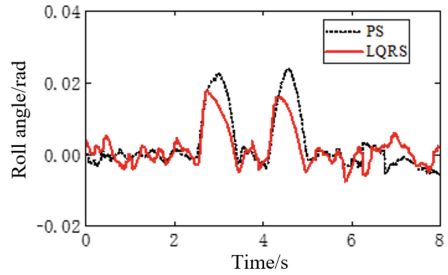
In order to further verify the accuracy of the above simulation results, the upper computer and Kvaser Light v2 control system are built. The sampling frequency are 100 Hz and the vehicle speed is 1 m/s. The parameter settings of the controller are consistent with the simulation for real, the results are shown in Fig. 12.



(a) Vertical acceleration



(b) Pitch angle



(c) Roll angle

Fig. 12. Experiment results of ATV attitude control

The ATV experiment results are shown in Table 7, the peak reduction ratio of pitch angle and roll angle are 20% and 25.94% respectively, and the rms value reduction ratio of those are 28.36% and 27.85% respectively, which means the attitude angle of the whole vehicle has been suppressed to some extent. Meanwhile, the reduction ratio of vertical displacement acceleration is between 12.65% and 17.99%, which indicates that the ride comfort of the whole vehicle has been enhanced to some extent.

Table 7. Comparison of attitude control experiment results

Performance indicators	Peak value			Rms value		
	PS	LQRS	Reduction ratio	PS	LQRS	Reduction ratio
vertical acceleration/(m/s ²)	4.1258	3.3837	17.99%	0.4711	0.4115	12.65%
pitch angle/rad	0.0180	0.0144	20.00%	0.0067	0.0048	28.36%
roll angle/rad	0.0239	0.0177	25.94%	0.0079	0.0057	27.85%

The comparisons are as shown in Fig. 13, which means the experimental improvements in peak and rms value of vertical acceleration, pitch angle, and roll angle are lower than those of the simulation, with a total average improvement that is 10% lower.

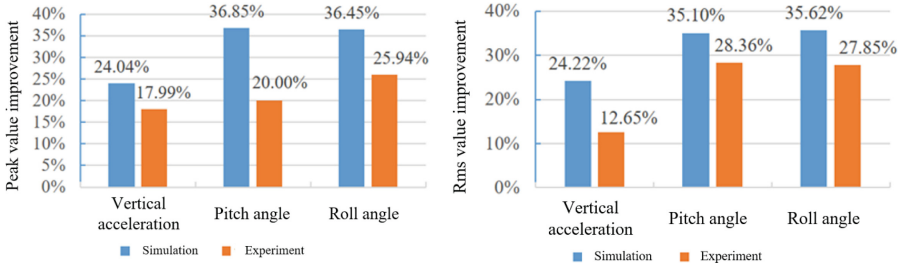


Fig. 13. Comparison of simulation and experiment improvement of LQR attitude control

The possibilities of the reduction of the improvement effect are analyzed, which include the lower accuracy of the established vehicle dynamic model due to the partial linear approximation, which leads to the poor performance of the designed LQR controller in the experiment; the delayed error of the electric servo actuator compared to the simulation; the high interfering noise of the sensors and other equipment in the experimental process.

6 Conclusion

In order to improve attitude control ability of all-terrain vehicles in complex terrain, a series active suspension all-terrain vehicle is taken as the research object, and a double closed-loop control strategy based on LQR controller is designed. Its main contents are as followed:

- 1) Through the simplification and linearization of the all-terrain vehicle model, the kinematics and dynamics analysis of each mechanism, and the introduction of second-order low-pass filter in the series active suspension, the difficulties in the speed control modeling of the electric servo actuator are solved, and the whole vehicle dynamic model of the series active suspension all-terrain vehicle is established.
- 2) Based on the vehicle dynamic model and the sensor system, the vehicle attitude is analyzed. And the vertical displacement excitation of each wheel is classified and calculated according to the kinematic relationship of the attitude and the pavement elevation information, so the terrain estimation model is obtained; considering the body vertical acceleration, dynamic travel of the passive suspension, dynamic displacement of the tires, roll angle and pitch angle, the optimal control law is solved by the Ricatti equation, and the LQR attitude controller is designed.
- 3) Three types of simulated terrain are established: bump pavement, sinusoidal wave pavement and random pavement, which are used to simulate real road conditions to verify the transient, stable state and random response characteristics of the control system respectively. Based on the dual-loop LQR attitude controller, the effectiveness

of the LQR attitude controller is validated by simulation and experiment, with the attitude control simulation improving by more than 35%, the ride comfort simulation improving by 24%, the experiment attitude improving by more than 20%, and the ride comfort experiment improving by 12%.

The accuracy of the established vehicle dynamic model will be further increased to improve the performance of the LQR controller in the future. In addition, there is also potentials for improvement because of the limitations of the electric servo actuator, the interfering noise of the sensors and other equipment.

Acknowledgements. This paper is supported by Projects in Jilin Scientific and Technological Development Program (No. YDZJ202101ZYTS190) and Scientific Research Planning Project of Jilin Provincial Department of Education (No. JJKH20190752SK). The authors would like to acknowledge the support of Changsha Automobile Innovation Research Institute, for providing the equipment and venues to carry out the experimental works.

References

1. Feng, Y., Xian, Q.: Development and application of testing system for vibration and ride comfort of all-terrain vehicle. *Noise Vibr. Worldwide* **50**(8), 239–244 (2019)
2. Chen, J., Cheng, J., Nie, Y.: Roll control of vehicle active suspension under steering condition. *Automot. Eng.* (5), 616–620 (2014)
3. Yao, J., Wang, M., Li, Z.H., Ren, S., Sun, N.: Research on automobile active roll control based on active suspension. *J. Mech. Strength* **40**(3), 534–539 (2018)
4. Liang, W., Ahmac, E., Khan, M.A., et al.: Integration of active tilting control and full-wheel steering control system on vehicle lateral performance. *Int. J. Automot. Technol.* **22**, 979–992 (2021)
5. Meng, A., Wang, L., Yang, J.: A study on slow-active suspension system based on output-feedback control. *Veh. Power Technol.* (003), 36–40 (2002)
6. van der Westhuizen, S.F., Els, P.S.: Slow active suspension control for rollover prevention. *J. Terrramech.* **50**(1), 29–36 (2013)
7. Saibal, M., et al.: Ant colony optimization tuned closed-loop optimal control intended for vehicle active suspension system. *IEEE Access* **10**, 53735–53745 (2022)
8. Pang, H., Iang, J., Wang, J.: Adaptive fuzzy sliding mode control for vehicle active suspension systems considering system uncertainty. *J. Vibr. Shock* **37**(15), 261–269 (2018)
9. Elmadany, M.M., Al Bassam, B.A., Fayed, A.A.: Preview control of slow-active suspension systems. *J. Vibr. Control* **17**(2), 245–258 (2011)
10. Patra, A.K., Mishra, A.K., Agrawal, R.: Fuzzy logic controller design for stabilizing and trajectory tracking of vehicle suspension system. *Smart Innov. Syst. Technol.* **194**, 575–587 (2021)
11. Gu, C., Yin, J., Chen, X.: Robust control and optimization of a rocker-pushrod electromagnetic active suspension. *Automot. Eng.* **40**(1), 34–40 (2018)
12. Du, M.M., Zhao, D.X., Yang, B., et al.: Terminal sliding mode control for full vehicle active suspension systems. *J. Mech. Sci. Technol.* **32**(6), 2851–2866 (2018)
13. Taghavifar, H.: Reduced vibration of off-road vehicle nonlinear suspension system using an adaptive integral sliding mode-neural network controller. *Int. J. Dyn. Control* **8**, 291–301 (2019)

14. Nguyen, T.A.: Control an active suspension system by using PID and LQR controller. *Int. J. Mech. Prod. Eng. Res. Dev.* **10**(3), 7003–7012 (2020)
15. ElMadany, M.M., Qarmoush, A.O.: Dynamic analysis of a slow-active suspension system based on a full car model. *J. Vib. ControlVib. Control* **17**(1), 39–53 (2011)
16. GB/T 4970-2009. Method of running test—Automotive ride comfort (1985)
17. Dai, H., Wang, X.: Simulation of PID control for intelligent rail vehicles under LQR optimization. *J. Qiqihar Univ. (Nat. Sci. Ed.)* **34**(2), 11–17 (2018)